 CMES, vol.2, no.2, pp.117-142, 2001

The Meshless Local Petrov-Galerkin (MLPG) Method for Solving Incompressible Navier-Stokes Equations

H. Lin and S.N. Atluri[1]

Abstract: The truly Meshless Local Petrov-Galerkin (MLPG) method is extended to solve the incompressible Navier-Stokes equations. The local weak form is modified in a very careful way so as to ovecome the so-called Babuška-Brezzi conditions. In addition, The upwinding scheme as developed in Lin and Atluri (2000a) and Lin and Atluri (2000b) is used to stabilize the convection operator in the streamline direction. Numerical results for benchmark problems show that the MLPG method is very promising to solve the convection dominated fluid mechanics problems.

keyword: MLPG, MLS, Babuška-Brezzi conditions, upwinding scheme, incompressible flow, Navier-Stokes equations.

1 Introduction

A number of numerical schemes has been used to solve the fluid flows. The finite difference method (FDM), the finite element method (FEM) and the finite volume method (FVM) have achieved a lot of success in computer modeling in fluid flows. However, their reliance on a mesh leads to complications for certain classes of problems. The generation of good quality meshes presents significant difficulties in the analysis of engineering systems (especially in 3D). These difficulties can be overcome by the so-called meshless methods, which have attracted considerable interest over the past decade. A number of meshless methods has been developed by different authors, such as Smooth Particle Hydrodynamics (SPH) [Lucy (1977)], Diffuse Element Method (DEM) [Nayroles, Touzot, and Villon (1992)], Element Free Galerkin method (EFG) [Belytschko, Lu, and Gu (1994)], Reproducing Kernel Particle Method (RKPM) [Liu, Jun, and Zhang (1995)], hp-clouds method [Duarte and Oden (1996)], Finite Point Method (FPM) [Oñate, Idelsohn, Zienkiewicz, and Taylor (1996)], Partition of Unity Method (PUM) [Babuška and Melenk (1997)], Local Boundary Integral Equation method (LBIE) [Zhu, Zhang, and Atluri (1998a,b)], Meshless Local Petrov-Galerkin method (MLPG) [Atluri and Zhu (1998a,b)]. Most of these methods with the exception of MLPG, LBIE, and FPM, in reality, are not really meshless methods, since they use a background mesh for the numerical integration of the weak form.

As discussed in Atluri, Kim, and Cho (1999), the MLPG method is based on a weak form computed over a local sub-domain and it is a truly meshless method. It offers a lot of flexibility to deal with different boundary value problems. A wide range of problems has been solved by Atluri and his coauthors. The MLPG method can also be easily extended to solve the fluid mechanics problems, due to its very general nature. In Lin and Atluri (2000a) and Lin and Atluri (2000b), convection-diffusion problems and nonlinear Burgers' equations have been solved by using the MLPG method. Results there show that it is very promising to use the MLPG method to solve more general fluid mechanics problems. In this paper, the solution of incompressible flows will be addressed.

As known, the main issues germane to the development of a successful solver for incompressible Navier-Stokes equations are: (i) proper treatment of the nonlinear convection term; and (ii) proper treatment of incompressibility. Improper treatments may result in spurious oscillations for velocity and/or pressure solutions. To deal with the first issue - nonlinear convection term, upwinding scheme is needed for high Reynolds number flows. In Lin and Atluri (2000a) and Lin and Atluri (2000b), simple and novel upwinding schemes have been introduced into the MLPG method. Similar ideas can be used to deal with Navier-Stokes flows. For the second issue, a more careful consideration is needed for the MLPG method.

In general, incompressible flows can be solved by using both primitive and derived (such as vorticity and

[1] Center for Aerospace Research and Education, 7704 Boelter Hall, University of California, Los Angeles, CA 90095-1600

stream function) variables. The approaches based on derived variables, such as vorticity-stream function and dual-potential methods, can satisfy the incompressibility condition automatically, and the pressure is eliminated, but these methods lose some of their attractiveness when applied to a 3-D flow. Consequently, the incompressible N-S equations are most often solved by the methods based on primitive variables for 3-D problems. Even for 2-D problems, the use of primitive variables is quite common, especially when robust codes are needed for various applications. Therefore, methods based on primitive variables are considered here.

For methods based on primitive variables, in order to incooperate the incompressibility constraint, the so-called mixed formulations will be obtained by introducing another variable, the Lagrange multiplier. It is well known that there are governing stability conditions for this kind of mixed formulations. Babuška (1971) and Brezzi (1974) have established these conditions, usually referred to as the Babuška-Brezzi conditions. In practice, it is not easy to satisfy the Babuška-Brezzi conditions for usual numerical schemes. As known, when a non-staggered grid is used in FDM, or, equal-order interpolations are used in FEM, it leads to algebraic systems with singular coefficient matrices that contain too many zero eigenvalues. Consequently, the resulting pressure solution is contaminated with pressure modes and is grossly erroneous. To avoid this problem, for FDM, staggered grids are adopted in which the nodal velocity components and the pressure are placed in different locations; for FEM, mixed-order interpolations, which try to satisfy the inf-sup conditions of Babuška and Brezzi, have to be chosen very carefully.

For meshless methods based on mixed formulations, the same problems will arise from the treatment of incompressibility constraint. As known, very few studies have been performed by using meshless methods, to solve incompressible flows. In this paper, we solve incompressible N-S equations by using the MLPG method. Since the MLPG method is based on local weak form, and usually the standard Galerkin procedure is used, the ways to deal with the Babuška-Brezzi conditions in FEM should be good guides for proposing the approaches in the MLPG method, to cope with the incompressibility constraint.

In FEM, several different approaches have been used to deal with the incompressibility constraint. As mentioned above, mixed-order interpolations may be used, see, e.g., Fortin (1981), Oden and Jacquotte (1984), Stenberg (1984), and etc., but it is difficult to choose proper interpolations, and may not make sure that the Babuška-Brezzi conditions are satisfied. So certain "cures" and "smoothing techniques" for generating "good" pressure solutions may be necessary. Another way is to use the so-called "selective-reduced-integration-penalty" (SRIP) methods. In this approach, the constitutive equation is modified through the introduction of a penalty parameter and the pressure is eliminated ab-initio from the formulation but is computed by post-processing the obtained velocity solutions, see, e.g., Malkus and Hughes (1978), Hughes, Liu, and Brooks (1979), Oden, Kikuchi, and Song (1982), and etc. Just as in the mixed-order approach, this may not satisfy the Babuška-Brezzi conditions and the selective reduced integration is not practical for the MLPG method. One alternative approach is to introduce the deviatoric stress as an additional variable, as done in Bratianu and Atluri (1983) and Yang and Atluri (1984a,b). This method works well for incompressible flows, but it is not easy to choose the interpolations for the deviatoric stress and additional variables cause additional cost.

In the last decade, two more general methods were proposed and became more and more popular: one is to use the classical FEM method with standard piecewise polynomials enriched by bubble functions, see Brezzi, Bristeau, Franca, Mallet, and Roge (1992), Franca and Russo (1996), Franca, Nesliturk, and Stynes (1998) and references therein; the other is to modify the mixed formulations by adding approximate 'perturbation' terms based on residual forms of the Euler-Lagrange equations in order to enhance the stability without upsetting consistency, see, e.g., Hughes and Franca (1987), Franca and Hughes (1988), Pierre (1988), Douglas and Wang (1989), Franca and Frey (1992), and etc. These two methods could be related to each other (see Brezzi, Bristeau, Franca, Mallet, and Roge (1992)). In practice, the sencond one is more general and easier to implement than the first one and thus more popular, although some parameters have to be tuned. In addition, it is not convenient to extend the first method to the MLPG method. For the second method, this kind of extension is very straightforward. In this paper, one kind of this idea, modifying the standard mixed formulations to circumvent the Babuška-Brezzi conditions, will be introduced for the MLPG method, and numerical tests will be performed.

2 Incompressible Navier-Stokes Equations and the Local Weak Form

The steady-state incompressible Navier-Stokes equations can be written as:

$$u_j\frac{\partial u_i}{\partial x_j}+\frac{\partial p}{\partial x_i}-\frac{2}{Re}\frac{\partial \varepsilon_{ij}}{\partial x_j}-f_i=0 \tag{1}$$

$$\frac{\partial u_i}{\partial x_i}=0 \tag{2}$$

where, u_i is the velocity, p is the pressure, f_i is the body force, Re is the Reynolds number, and $\varepsilon_{ij}=u_{(i,j)}=\frac{1}{2}(\frac{\partial u_i}{\partial x_j}+\frac{\partial u_j}{\partial x_i})$. Eq. (1) and Eq. (2) are the momentum equations and the continuity equation.

The boundary conditions can be assumed to be:

- Dirichlet Boundary Conditions:

$$u_i=\overline{u}_i \quad on \quad \Gamma_u \tag{3}$$

- Neumann Boundary Conditions:

$$\left(\frac{2}{Re}\varepsilon_{ij}-p\delta_{ij}\right)n_j=\overline{t}_i \quad on \quad \Gamma_t \tag{4}$$

where, $\overline{u}_i$ and $\overline{t}_i$ are given, n_j is the outward unit normal vector to Γ, Γ_u and Γ_t are subsets of Γ satisfying $\Gamma_u\cap\Gamma_t=\emptyset$ (the empty set) and $\Gamma_u\cup\Gamma_t=\Gamma$.

The MLPG method is based on a local weak form computed over a local sub-domain, which can be any simple geometry like a sphere, cube or ellipsoid in 3D. To obtain the local weak form for N-S equations, Eq. (1) and Eq. (2 can be weighted by test functions w_i and q respectively and integrated over a local sub-domain Ω_s, such that the following equations are obtained:

$$\int_{\Omega_s}\left(u_j\frac{\partial u_i}{\partial x_j}+\frac{\partial p}{\partial x_i}-\frac{2}{Re}\frac{\partial \varepsilon_{ij}}{\partial x_j}-f_i\right)w_i\,d\Omega=0 \tag{5}$$

$$\int_{\Omega_s}\frac{\partial u_i}{\partial x_i}q\,d\Omega=0 \tag{6}$$

for all w_i and q. By using the integration by parts, Eq. (5) is recast into a local weak form as:

$$\int_{\Omega_s}\left(u_j\frac{\partial u_i}{\partial x_j}w_i-p\frac{\partial w_i}{\partial x_i}+\frac{2}{Re}\varepsilon_{ij}\frac{\partial w_i}{\partial x_j}-f_iw_i\right)d\Omega - \int_{\Gamma_s}\left(\frac{2}{Re}\varepsilon_{ij}-p\delta_{ij}\right)n_jw_i\,d\Gamma=0 \tag{7}$$

for all continuous trial functions u_i and continuous test functions w_i. By imposing the boundary conditions in a weak sense, the local weak form Eq. (7) can be rewritten as:

$$\int_{\Omega_s}\left(u_j\frac{\partial u_i}{\partial x_j}w_i-p\frac{\partial w_i}{\partial x_i}+\frac{2}{Re}\varepsilon_{ij}\frac{\partial w_i}{\partial x_j}-f_iw_i\right)d\Omega - \int_{\Gamma_{sI}}\left(\frac{2}{Re}\varepsilon_{ij}-p\delta_{ij}\right)n_jw_i\,d\Gamma-\int_{\Gamma_{su}}\left(\frac{2}{Re}\varepsilon_{ij}-p\delta_{ij}\right)n_jw_i\,d\Gamma - \int_{\Gamma_{st}}\left(\frac{2}{Re}\varepsilon_{ij}-p\delta_{ij}\right)n_jw_i\,d\Gamma=0 \tag{8}$$

where, Γ_{sI} is the part of Γ_s inside the global domain, $\Gamma_{su}=\Gamma_s\cap\Gamma_u$, and $\Gamma_{st}=\Gamma_s\cap\Gamma_t$.

So far, the formulations are based on mixed-form. The standard Lagrange multiplier is used to impose the incompressibility constraints. As known, there are the so-called Babuška-Brezzi stability conditions for this kind of formulations. If these conditions are not satisfied, spurious pressure solutions may be obtained. There are several approaches to solve this problem as discussed in the introduction, but the most straightforward approach is to modify the standard mixed formulations by adding approximate 'perturbation' terms based on residual forms of the Euler-Lagrange equations. To implement this approach in the MLPG method, Eq. (6) can be modified by adding a 'perturbation' term as following:

$$\int_{\Omega_s}\frac{\partial u_i}{\partial x_i}q\,d\Omega+\tau\int_{\Omega_s}\left(u_j\frac{\partial u_i}{\partial x_j}+\frac{\partial p}{\partial x_i}-\frac{2}{Re}\frac{\partial \varepsilon_{ij}}{\partial x_j}-f_i\right)\times\frac{\partial q}{\partial x_i}\,d\Omega=0 \tag{9}$$

where, τ is the stability parameter. By choosing τ carefully, the stability problem can be solved without upsetting the consistency.

Similar to what being done in the stabilized FEM methods, see, e.g., Pierre (1988), Franca and Frey (1992), and etc., τ may be defined as:

$$\tau=\begin{cases}\beta D^2 & Re_L<1\\ \frac{D}{2||\mathbf{u}||} & Re_L\geq 1\end{cases} \tag{10}$$

where, $D=2r$ is the diameter of support for the weight functions, $Re_L=D*||\mathbf{u}||*Re$ is local Reynolds numer related to local sub-domain, and $||\mathbf{u}||=(u_iu_i)^{1/2}$. When this formula for τ is used, we are left with the problem of setting parameter β correctly. It may depend on the size of local sub-domain and the global Reynolds number

Re. This is still an open problem. More investigation is needed.

In the implementation, the term related to the second order derivative ($\frac{2}{Re}\frac{\partial \varepsilon_{ij}}{\partial x_j}$) in Eq. (9) will be ignored, because this term is not that important, especially for the linear basis functions, and additional cost is required to calculate the second order derivative of the shape functions (Similar idea was once used by Nayroles, Touzot, and Villon (1992) to reduce the cost.) This will be studied by numerical examples.

In practice, to solve the boundary value problems, one can randomly put nodes in the domain Ω and construct the local weak form for each node. Theoretically, as long as the union of all local sub-domains covers the whole domain Ω, i.e., $\cup\Omega_s \supset \Omega$, Eq. (1) and Eq. (2) will be satisfied, a posteriori, in the global domain Ω.

3 The Moving Least Square (MLS) approximation scheme

As in general numerical simulation methods, the MLPG method needs some kind of interpolation schemes and discetization methods to generate the algebraic systems, which can be solved numerically. In order to preserve the local character of the numerical implementation, the interpolation schemes should have the local property. There are different approaches to achieve this aim. In general, instead of using traditional non-overlapping, continguous meshes to form the interpolation scheme, a meshless method uses a local interpolation or approximation to represent the trial/test functions with the values (or the fictitious values) of the unknown variable at some randomly located nodes. There is a number of local interpolation schemes, such as MLS, PUM, RKPM, hp-clouds, Shepard function, etc., available for this purpose. The work done by Babuška and Melenk (1997) has shown that most meshless interpolation schemes belong to the partition of unity family and have similar features. The Moving Least Square (MLS) method is one of them and is generally considered as one of the schemes to interpolate data with a reasonable accuracy. Therefore, the MLS scheme is used in this paper.

Consider the approximation of a function $u(\mathbf{x})$ in a domain Ω with a number of scattered nodes $\{\mathbf{x}_i\}$, $i = 1,2,\ldots,n$, the moving least-square approximant $u^h(\mathbf{x})$ of $u(\mathbf{x})$, $\forall \mathbf{x} \in \Omega$, can be defined by

$$u^h(\mathbf{x}) = \mathbf{p}^T(\mathbf{x})\mathbf{a}(\mathbf{x}) \quad \forall \mathbf{x} \in \Omega \tag{11}$$

where, $\mathbf{p}^T(\mathbf{x}) = [p_1(\mathbf{x}), p_2(\mathbf{x}), \ldots, p_m(\mathbf{x})]$ is a complete monomial basis of order m, which, for example, can be chosen as linear:

$$\mathbf{p}^T(\mathbf{x}) = [1, x, y], \quad m = 3; \tag{12}$$

or quadratic:

$$\mathbf{p}^T(\mathbf{x}) = [1, x, y, x^2, xy, y^2], \quad m = 6 \tag{13}$$

for 2D problems, and $\mathbf{a}(\mathbf{x})$ is a vector containing coefficients $a_j(\mathbf{x})$, $j = 1,2,\ldots,m$ which are functions of the space coordinates $\mathbf{x}$, and determined by minimizing a weighted discrete L_2 norm, defined as:

$$\begin{aligned} \mathbf{J}(\mathbf{x}) &= \sum_{i=1}^{n} w_i(\mathbf{x})[\mathbf{p}^T(\mathbf{x}_i)\mathbf{a}(\mathbf{x}) - \hat{u}_i]^2 \\ &= [\mathbf{P}\cdot\mathbf{a}(\mathbf{x}) - \hat{\mathbf{u}}]^T \cdot \mathbf{W} \cdot [\mathbf{P}\cdot\mathbf{a}(\mathbf{x}) - \hat{\mathbf{u}}] \end{aligned} \tag{14}$$

where $w_i(\mathbf{x})$ is the weight function associated with the node i, with $w_i(\mathbf{x}) > 0$ for all $\mathbf{x}$ in the support of $w_i(\mathbf{x})$, $\mathbf{x}_i$ denotes the value of $\mathbf{x}$ at node i, n is the number of nodes in Ω for which the weight functions $w_i(\mathbf{x}) > 0$, the matrices $\mathbf{P}$ and $\mathbf{W}$ are defined as

$$\mathbf{P} = \begin{bmatrix} \mathbf{p}^T(\mathbf{x}_1) \\ \mathbf{p}^T(\mathbf{x}_2) \\ \cdots \\ \mathbf{p}^T(\mathbf{x}_n) \end{bmatrix}_{n\times m} \tag{15}$$

$$\mathbf{W} = \begin{bmatrix} w_1(\mathbf{x}) & \cdots & 0 \\ \cdots & \cdots & \cdots \\ 0 & \cdots & w_n(\mathbf{x}) \end{bmatrix} \tag{16}$$

and

$$\hat{\mathbf{u}}^T = [\hat{u}_1, \hat{u}_2, \ldots, \hat{u}_n] \tag{17}$$

where, $\hat{u}_i, i = 1,2,\ldots,n$ are the fictitious nodal values and not the nodal values of the unknown trial function $u^h(\mathbf{x})$ in general.

The stationarity of $\mathbf{J}$ in Eq. (14) with respect to $\mathbf{a}(\mathbf{x})$ leads to the following relation between $\mathbf{a}(\mathbf{x})$ and $\hat{\mathbf{u}}$:

$$\mathbf{A}(\mathbf{x})\mathbf{a}(\mathbf{x}) = \mathbf{B}(\mathbf{x})\hat{\mathbf{u}} \tag{18}$$

where the matrices $\mathbf{A}(\mathbf{x})$ and $\mathbf{B}(\mathbf{x})$ are defined by

$$\mathbf{A}(\mathbf{x}) = \mathbf{P}^T\mathbf{W}\mathbf{P} = \sum_{i=1}^{n} w_i(\mathbf{x})\mathbf{p}(\mathbf{x}_i)\mathbf{p}^T(\mathbf{x}_i) \tag{19}$$

$$\begin{aligned} \mathbf{B}(\mathbf{x}) = \mathbf{P}^T\mathbf{W} = [&w_1(\mathbf{x})\mathbf{p}(\mathbf{x}_1), w_2(\mathbf{x})\mathbf{p}(\mathbf{x}_2), \ldots, \\ &w_n(\mathbf{x})\mathbf{p}(\mathbf{x}_n)] \end{aligned} \tag{20}$$

Solving this for $\mathbf{a}(\mathbf{x})$ and substituting it into Eq. (11), we get the MLS approximation as

$$u^h(\mathbf{x}) = \mathbf{\Phi}^T(\mathbf{x}) \cdot \hat{\mathbf{u}} = \sum_{i=1}^{n} \phi_i(\mathbf{x}) \hat{u}_i \quad \forall \mathbf{x} \in \Omega \tag{21}$$

where, the nodal shape function corresponding to nodal point $\mathbf{x}_i$ is given by

$$\mathbf{\Phi}^T(\mathbf{x}) = \mathbf{p}^T(\mathbf{x}) \mathbf{A}^{-1}(\mathbf{x}) \mathbf{B}(\mathbf{x}) \tag{22}$$

It should be noted that the MLS approximation is well defined only when the matrix $\mathbf{A}$ in Eq. (18) is non-singular. It can be seen that this is the case if and only if the rank of $\mathbf{P}$ equals m. A necessary condition for a well-defined MLS approximation is that at least m weight functions are non-zero (i.e. $n \geq m$) for each sample point $\mathbf{x} \in \Omega$ and that the nodes in Ω will not be arranged in a special pattern such as on a straight line.

The partial derivatives of $\phi_i(\mathbf{x})$ can be obtained as

$$\phi_{i,k} = \sum_{j=1}^{m} [p_{j,k}(\mathbf{A}^{-1}\mathbf{B})_{ji} + p_j(\mathbf{A}^{-1}\mathbf{B}_{,k} + \mathbf{A}^{-1}_{,k}\mathbf{B})_{ji}] \tag{23}$$

in which $\mathbf{A}^{-1}_{,k}$ is given by

$$\mathbf{A}^{-1}_{,k} = -\mathbf{A}^{-1}\mathbf{A}_{,k}\mathbf{A}^{-1} \tag{24}$$

and the index following a comma indicates a spatial derivative.

It is known that the smoothness of the shape functions $\phi_i(\mathbf{x})$ is determined by that of the basis functions and of the weight functions. Let $C^k(\Omega)$ be the space of k-th continuously differentiable functions. If $w_i(\mathbf{x}) \in C^k(\Omega), i = 1,2,\ldots,n$ and $p_j(\mathbf{x}) \in C^l(\Omega), j = 1,2,\ldots,m$, then $\phi_i(\mathbf{x}) \in C^r(\Omega)$ with $r = min(k,l)$. A number of choices are available for the basis functions and the weight functions. In this paper, the linear basis is chosen and a spline weight function as in Atluri and Zhu (1998a) is used:

$$w_i(\mathbf{x}) = \begin{cases} 1 - 6(\frac{d_i}{r_i})^2 + 8(\frac{d_i}{r_i})^3 - 3(\frac{d_i}{r_i})^4 & 0 \leq d_i \leq r_i \\ 0 & d_i \geq r_i \end{cases} \tag{25}$$

where $d_i = |\mathbf{x} - \mathbf{x}_i|$ is the distance from node $\mathbf{x}_i$ to point $\mathbf{x}$, and r_i is the size of the support for the weight function w_i. It can be easily seen that the spline weight function is C^1 continuous over the entire domain.

From the above discussion, it shows that the MLS shape functions don't have the Kronecker delta property. This causes the difficulty to impose the essential boundary conditions. Several methods have been proposed, e.g., see Belytschko, Krongauz, Organ, Fleming, and Krysl (1996) and Zhu and Atluri (1998). In this paper, the transformation method proposed by Atluri, Kim, and Cho (1999) are used to deal with the essential boundary conditions.

By using the MLS approximation scheme and dealing with boundary conditions, the discretization formulation of the local weak form can be easily obtained. Proper integration schemes are necessary to generate the algebraic equations. The local weak form provides a very clear concept for a local non-element integration, and leads to a natural way to construct the global stiffness matrix through the integration over a local sub-domain. Any kind of integratioon techniques, such as trapzoidal rule, Gaussian quadrature, and etc., can be used. So far, the computational cost is still high, because, in general, the shape functions obtained from meshless interpolation schemes are some complicated forms of rational functions, not simplely polynomial functions as those in the usual Galerkin Finite Element Method. Large number of integration points are required to obtain good accuracy. More discussions can be found in Atluri, Kim, and Cho (1999); Atluri, Cho, and Kim (1999). In this paper, Gaussian quadrature is used.

Further, due to the nonlinear convection term, the algebraic equations will be nonlinear. Some kind of iteration method to solve the algebraic equations is needed. The Newtonian iteration method will be used in this paper.

4 Upwinding Schemes

In fluid mechanics, the existence of the convection term makes the problem non-self-ajoint. A special treatment is needed to stabilize the numerical approximation for these kinds of problems. Schemes related to upwinding are the most general techniques to stabilize FDM, FEM and FVM. The same concept is needed in the meshless methods, so as to obtain a good accuracy for convection-dominated flows.

In Lin and Atluri (2000a), two upwinding schemes for the MLPG method have been developed and used to solve the convection-diffusion problems with high Peclet numbers. The results show that the Upwinding Scheme II

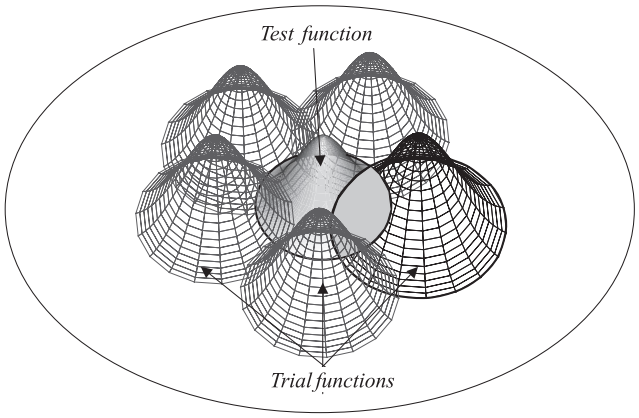

Figure 1 : The MLPG method without Upwinding.

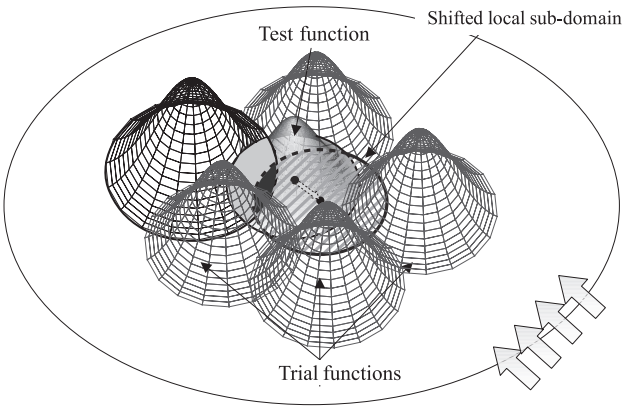

Figure 2 : MLPG Upwinding Scheme II (US-II).

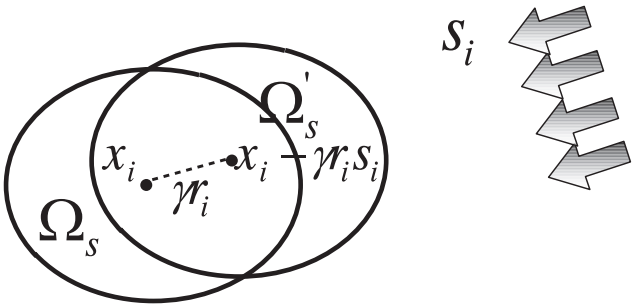

Figure 3 : MLPG Upwinding Scheme II (US-II): Specification.

(US-II) is a very good scheme, not only because it always gives good solutions, but also because of its very general nature. As discussed in Lin and Atluri (2000a), this scheme possesses the desirable feature to be a good upwinding scheme, which is, that upwinding effect should be applied only in the streamline direction and consistency for every term should be conserved. This kind of upwinding scheme has been extended to solve the nonlinear Burgers' equations successfully in Lin and Atluri (2000b). For Navier-Stokes equations, the similar idea will be used.

Because the MLPG method is based on a local weak form over a local sub-domain, it is very easy to include upwinding effects for Navier-Stokes equations. The general MLPG method is based on Petrov-Galerkin weighting procedures. Different spaces for the test and trial functions can be used, as shown in Fig. 1.

One simple way to include the upwinding effects can be done as in Lin and Atluri (2000a) and Lin and Atluri (2000b). One can easily shift the local sub-domain opposite to the streamline direction, as shown in Fig.2. The same spaces for the trial and test functions are used, that is, the same support and the same interpolation scheme (MLS) for the trial functions and the test functions are employed. We don't need to modify the local weak form. What we need to do is to move the local sub-domain when integration is implemented.

Here, the local sub-domain at $\mathbf{x}_i$ is no longer coincident with the support for the test functions at $\mathbf{x}_i$, but the size is the same. (It should be noted that in the usual MLPG method, we usually choose the test functions such that the integration term along the boundary Γ_{sI} equals to zero, but, in general, this is not true for the MLPG method with US-II. Therefore, in the local weak form, the integration term along the boundary Γ_{sI} should be retained.)

In particular, the distance of shift of the local sub-domain can be specified as γr_i, where, r_i is the size of the support for the test functions, which is equal to the size of the local domain, at $\mathbf{x}_i$, and γ is given by

$$\gamma = \coth(\frac{Re_L}{2}) - \frac{2}{Re_L} \tag{26}$$

in which Re_L is a local Reynolds number, defined as:

$$Re_L = 2||\mathbf{u}|| * r_i * Re \tag{27}$$

where, $||\mathbf{u}|| = \sqrt{u^2+v^2}$ in 2D. The direction of the shifting is opposite to the streamline direction $\mathbf{s}_i$ at $\mathbf{x}_i$, as shown in Fig.3.

For convenience, we denote this as Upwinding Scheme II (US-II) as before.

5 Numerical Examples

In this section, Stokes flow problems are solved to illustrate that the approach developed here is effective to overcome the Babuška-Brezzi conditions, and the general incompressible N-S equations are calculated, alternatively, by using the MLPG method without upwinding (MLPG) and by the MLPG method with Upwinding Scheme II (MLPG2).

5.1 Stokes Flows

For Stokes flows, there is no nonlinear convection term. Therefore, no iteration and upwinding schemes are needed. The modified formulation Eq. (9) with Eq. (8) is solved. Different values of β in Eq. (10) are chosen for the purpose of comparison.

5.1.1 A body force problem

This problem was suggested by Sani, Gresho, Lee, and Griffiths (1981). For an appropriate (polynomial) body force, the solution of the Stokes problem with homogeneous boundary conditions will be

$$u_1 = 2x^2(1-x)^2y(1-y)(1-2y) \tag{28}$$

$$u_2 = -2x(1-x)(1-2x)y^2(1-y)^2 \tag{29}$$

$$p = x^2 - y^2 \tag{30}$$

This solution is very smooth. It is a good example to assess the effectiveness of numerical schemes for Stokes flows. The exact solutions for velocity and pressure fields are plotted in Fig.4 with 11×11 points.

Different values of β are used and results are shown in Fig.5-Fig.10 for the MLPG method with 11×11 points and radius of support $r = 1.3h$ (h is the nodal distance).

From Fig. 5, it is obvious that the pressure solution is highly oscillatory when $\beta = 0$, i.e., when the standard mixed formulation is used. It shows that the best choice for β is $\beta = 0.01$. For smaller values of β, oscillations for pressure may persist, but for larger values of β, the boundary behaviour deteriorates the pressure solutions (at the corner near the origin where the pressure is too small). It also shows that, although the term related to the second order derivative ($\frac{2}{Re}\frac{\partial \varepsilon_{ij}}{\partial x_j}$) in Eq. (9) has been ignored in the calculation, the results are good enough. To consider the effect of the size of radius of support, Fig.11-Fig.16 show the results for the MLPG method with 11×11 nodes and radius of support $r = 2.1h$.

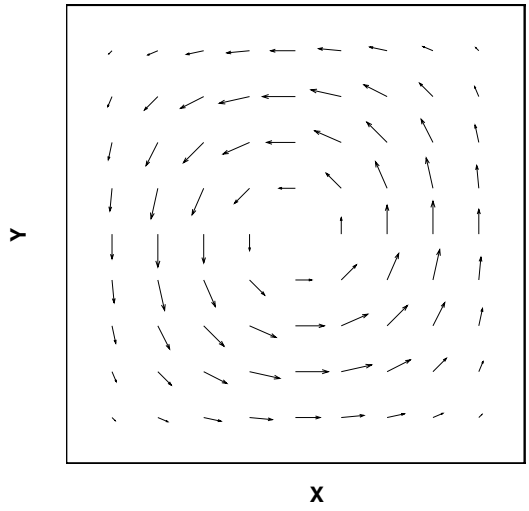

velocity field

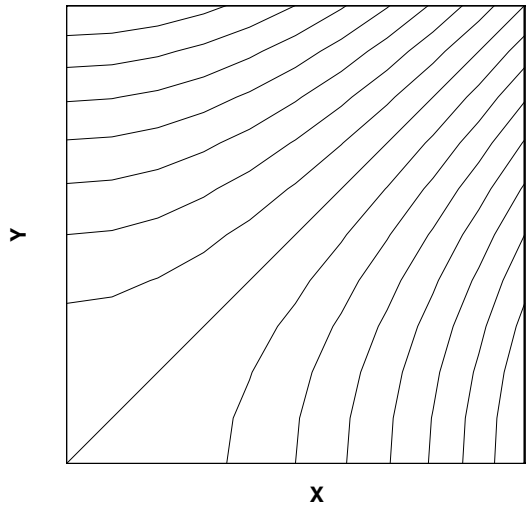

pressure contour

Figure 4 : A body force problem: exact solutions (11×11 nodes).

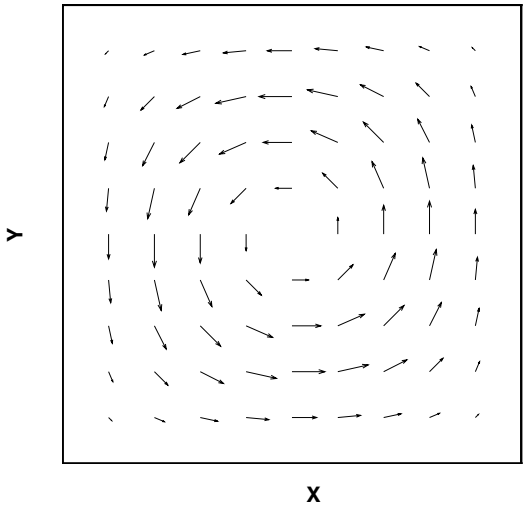

velocity field

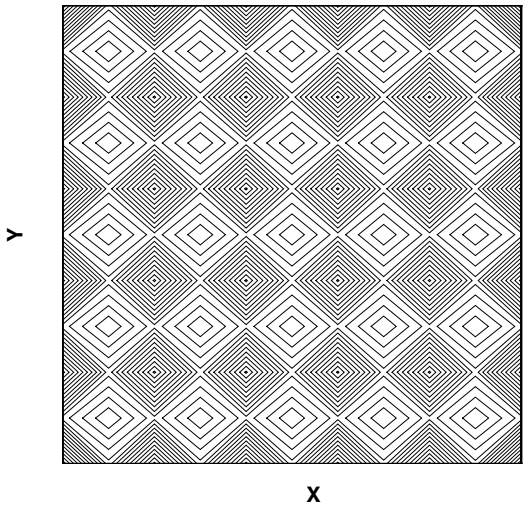

pressure contour

Figure 5 : A body force problem: MLPG with $\beta = 0$ (11×11 nodes and $r = 1.3h$).

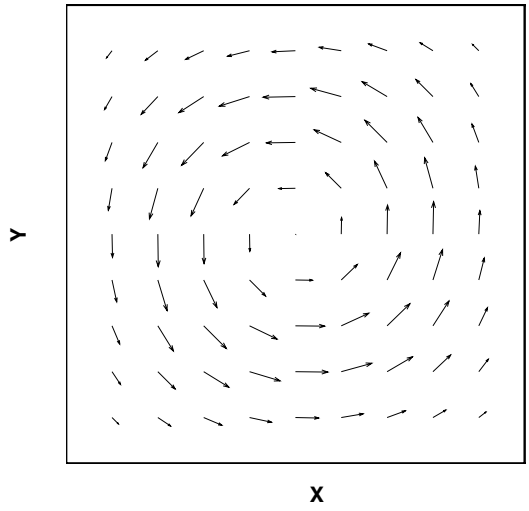

velocity field

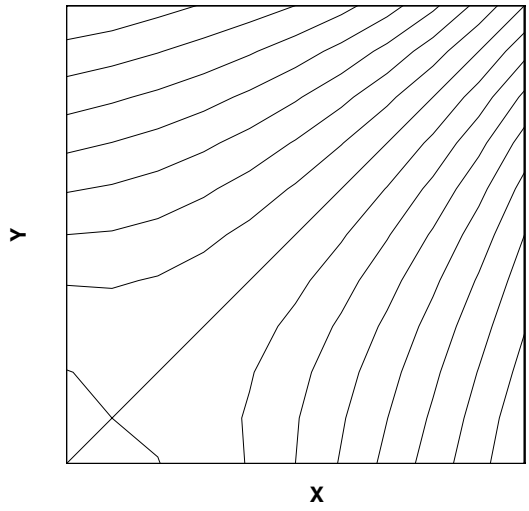

pressure contour

Figure 6 : A body force problem: MLPG with $\beta = 1$ (11×11 nodes and $r = 1.3h$).

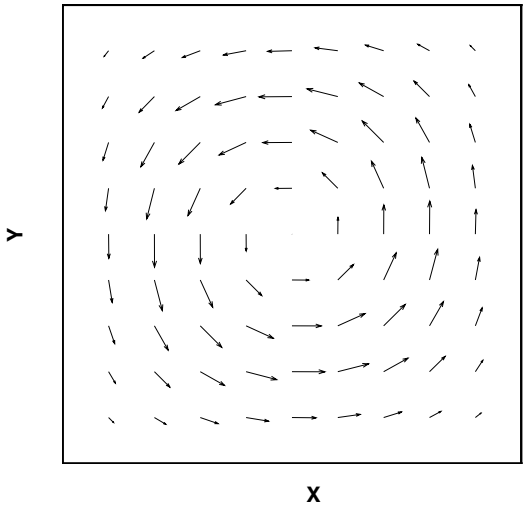

velocity field

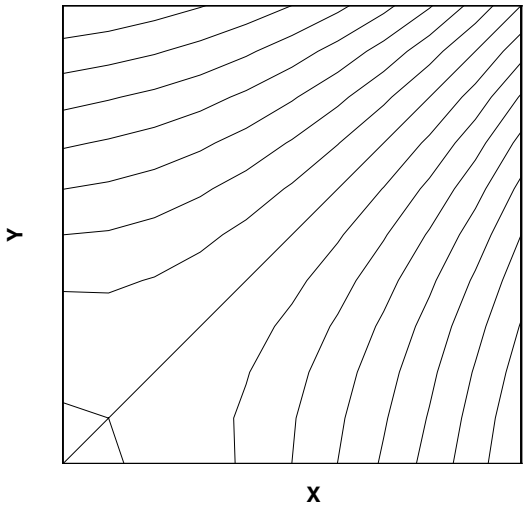

pressure contour

Figure 7 : A body force problem: MLPG with $\beta = 0.1$ (11×11 nodes and $r = 1.3h$).

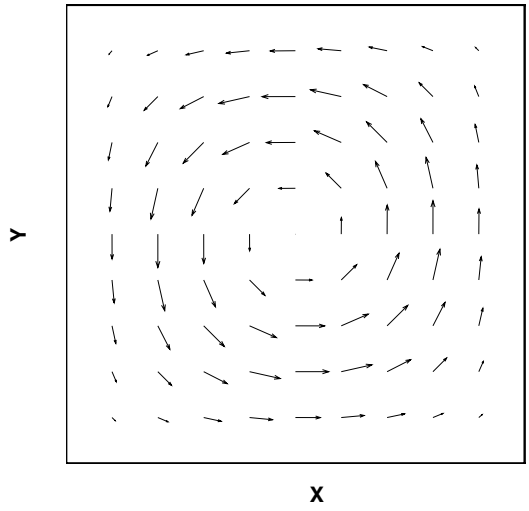

velocity field

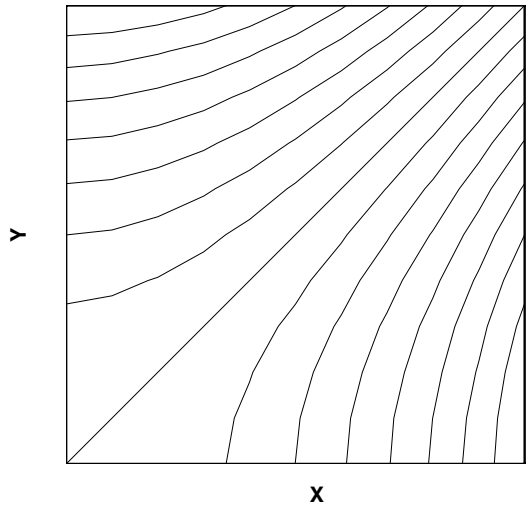

pressure contour

Figure 8 : A body force problem: MLPG with $\beta = 0.01$ (11×11 nodes and $r = 1.3h$).

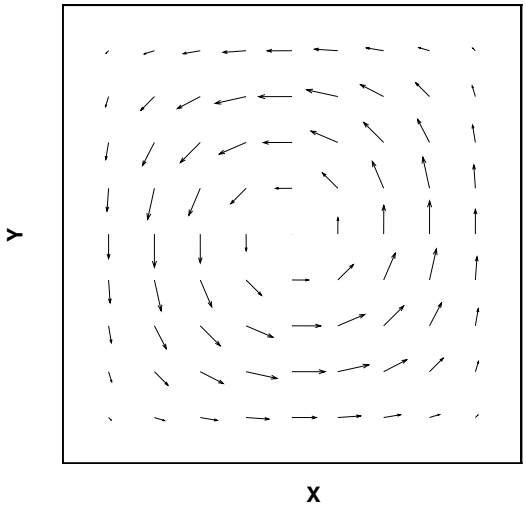

velocity field

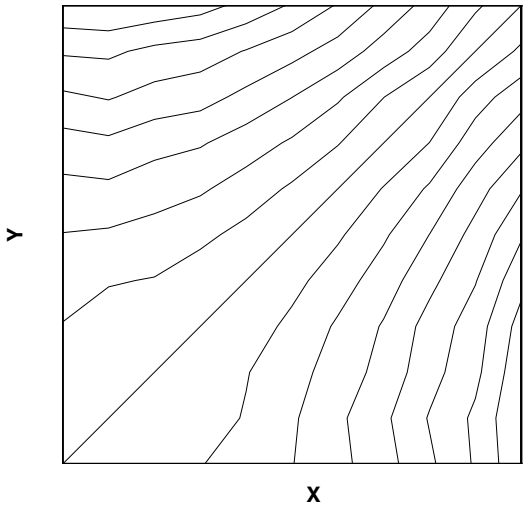

pressure contour

Figure 9 : A body force problem: MLPG with $\beta = 0.001$ (11×11 nodes and $r = 1.3h$).

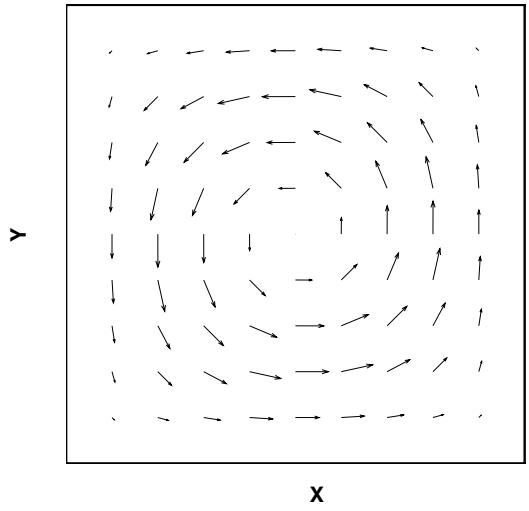

velocity field

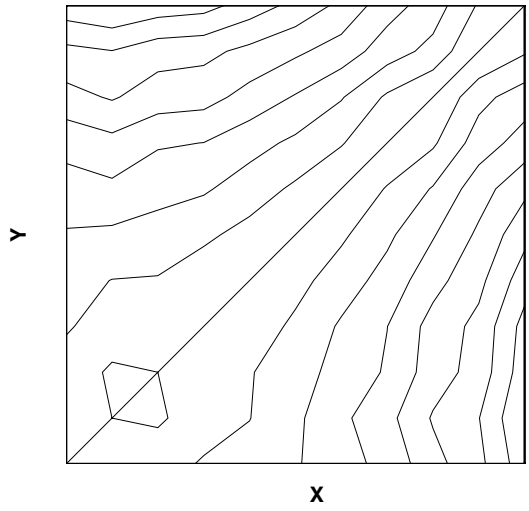

pressure contour

Figure 10 : A body force problem: MLPG with $\beta = 0.0001$ (11×11 nodes and $r = 1.3h$).

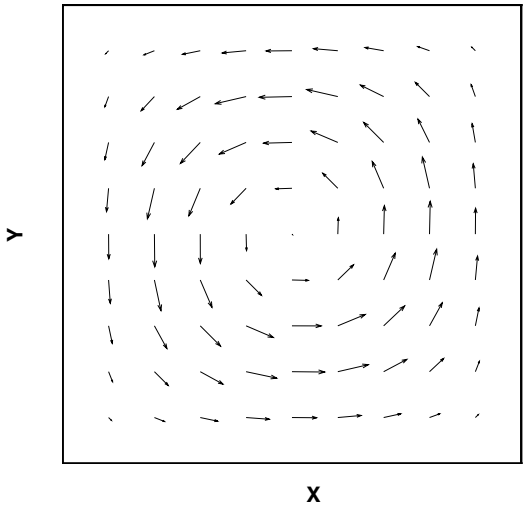

velocity field

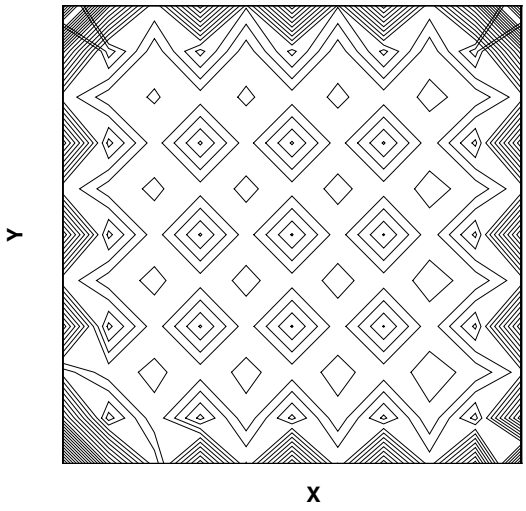

pressure contour

Figure 11 : A body force problem: MLPG with $\beta = 0$ (11×11 nodes and $r = 2.1h$).

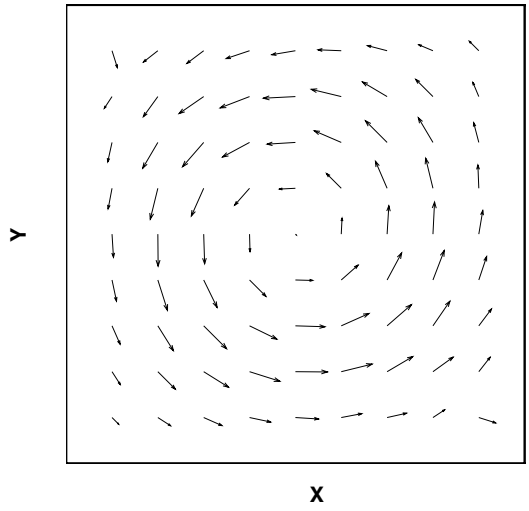

velocity field

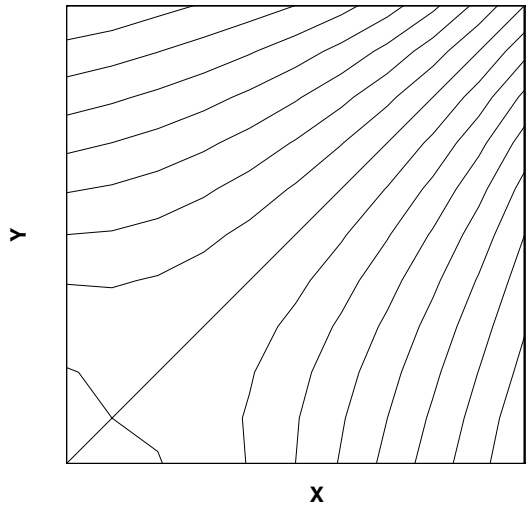

pressure contour

Figure 12 : A body force problem: MLPG with $\beta = 1$ (11×11 nodes and $r = 2.1h$).

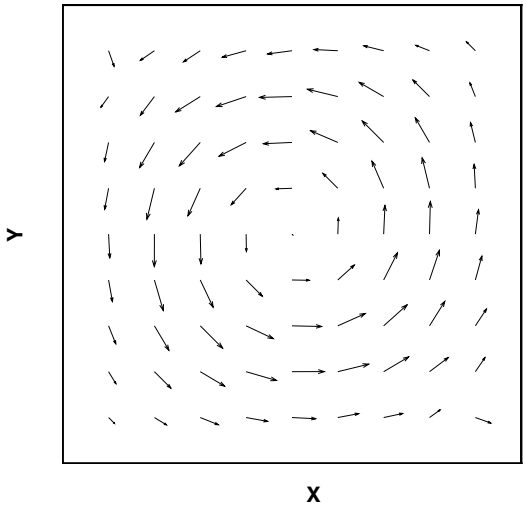

velocity field

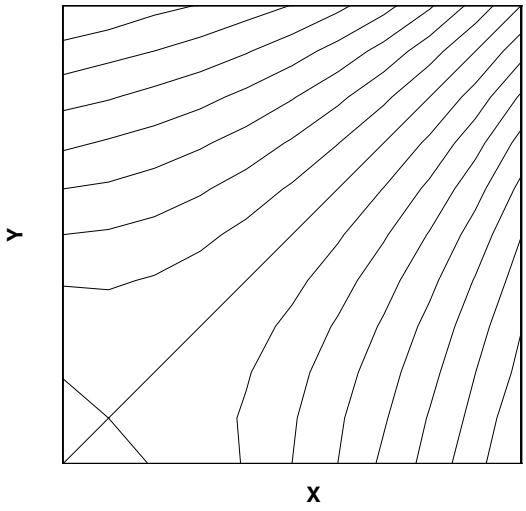

pressure contour

Figure 13 : A body force problem: MLPG with $\beta = 0.1$ (11×11 nodes and $r = 2.1h$).

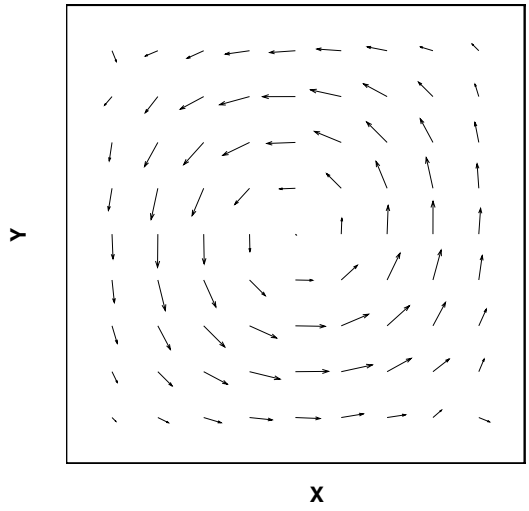

velocity field

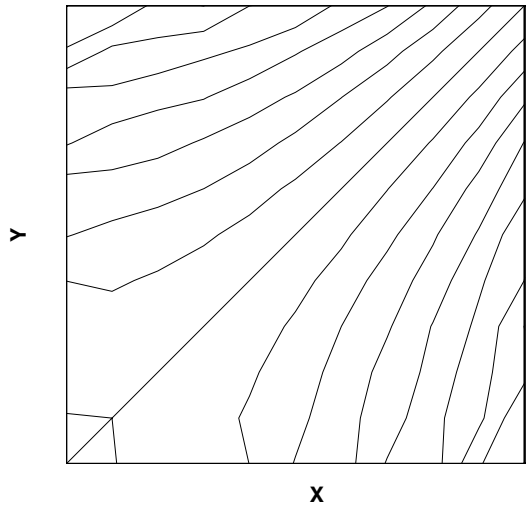

pressure contour

Figure 14 : A body force problem: MLPG with $\beta = 0.01$ (11×11 nodes and $r = 2.1h$).

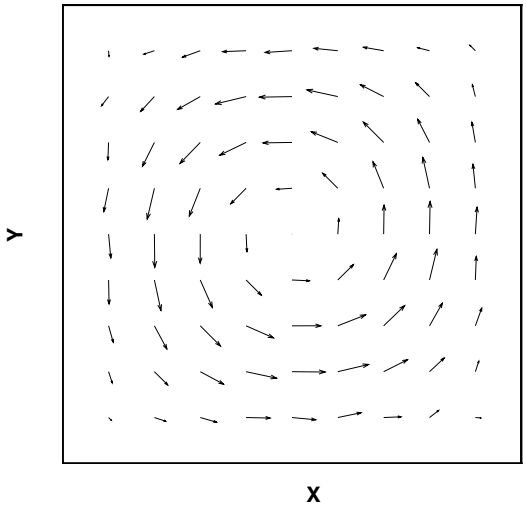

velocity field

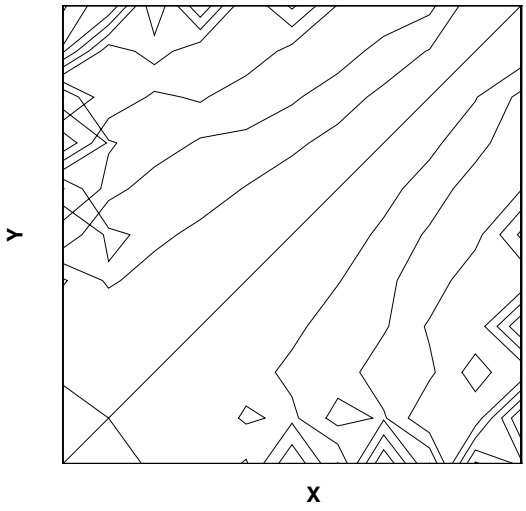

pressure contour

Figure 15 : A body force problem: MLPG with $\beta = 0.001$ (11×11 nodes and $r = 2.1h$).

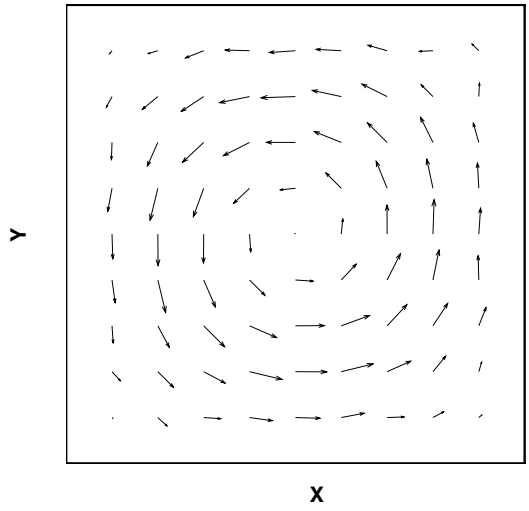

velocity field

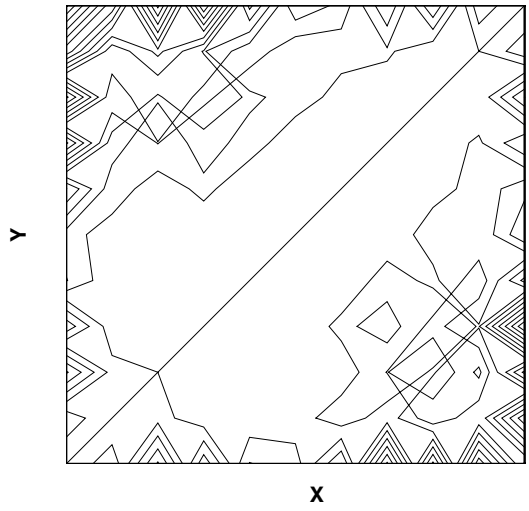

pressure contour

Figure 16 : A body force problem: MLPG with $\beta = 0.0001$ (11×11 nodes and $r = 2.1h$).

As before, if there is no modification for the mixed formulation, i.e., $\beta = 0$, the pressure solution is highly oscillatory although the velocity field solution appears satisfactory. When β becomes larger, the pressure oscillations becomes smaller. But, for too large a β, the boundary behaviour comes into effect (see at the corner near the origin where the pressure is too small). Compared with the previous results ($r = 1.3h$), it shows that, with larger radius support ($r = 2.1h$), it is not easy to say which value is the best choice for β. Both oscillations and boundary behaviour effect appear when $\beta = 0.01$. This difficulty may come from different reasons. One may arise from the ignored term (the second order derivative term in Eq. (9). When the radius of support becomes larger, this term may become more important. But it appears that this is not the quite reason, because when a proper β is used, one can obtain reasonably smooth pressure. The more reasonable explanation may be as follows: when a larger radius of support is used, the boundary behaviour takes more effect to the interior solutions; and the transformation method being used to impose the essential boundary conditions may make this effect stronger as already discussed in Lin and Atluri (2000a). A better imposition of essential boundary conditions, and a better choice for β may solve this problem.

Furthermore, to consider the effect of refinement, larger number of points are applied to recompute this problem. The exact solutions for velocity and pressure fields are plotted in Fig.17 with 21×21 points.

Again, different values of β are used and the results are shown in Fig.18-Fig.23 for the MLPG method with 21×21 points and radius of support $r = 1.3h$ (h is the nodal distance).

Fig.18 illustrates again that the MLPG method with the standard mixed formulation ($\beta = 0$) gives highly oscillatory pressure solutions even though the velocity field looks quite good. It also shows that ignoring the second order derivative term in Eq. (9) is quite reasonable. As in the case with fewer points, the best choice for β is $\beta = 0.01$.

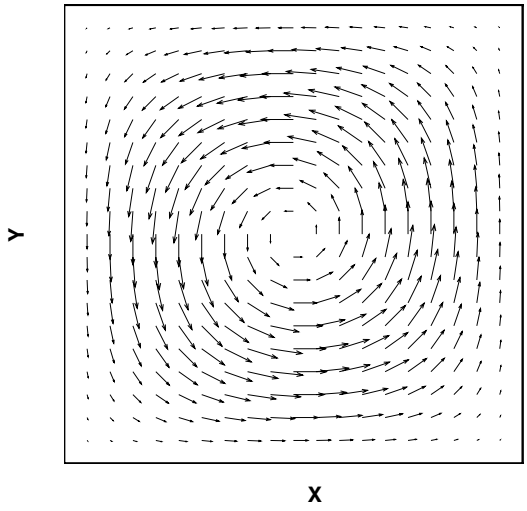

velocity field

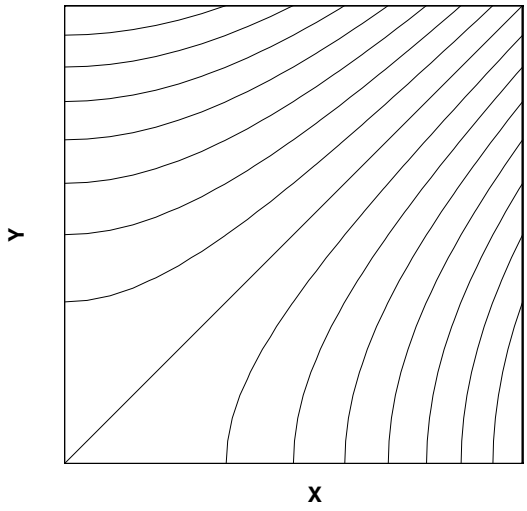

pressure contour

Figure 17 : A body force problem: exact solutions (21×21 nodes).

5.1.2 Lid-driven cavity flow

As an additional example, the results for the lid-driven cavity flow-through case are presented here. Unlike the preceding example, this one is known to be very stiff because of singular boundary conditions.

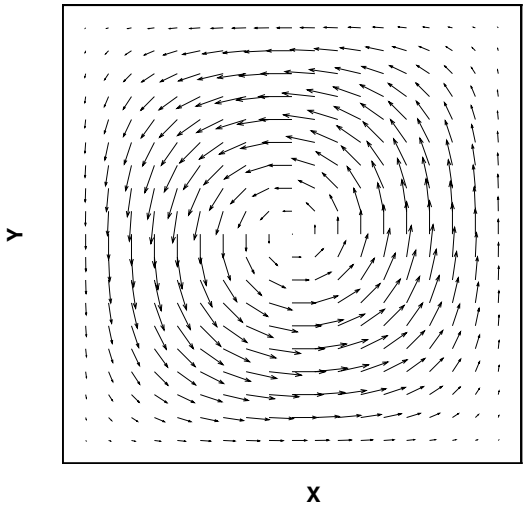

velocity field

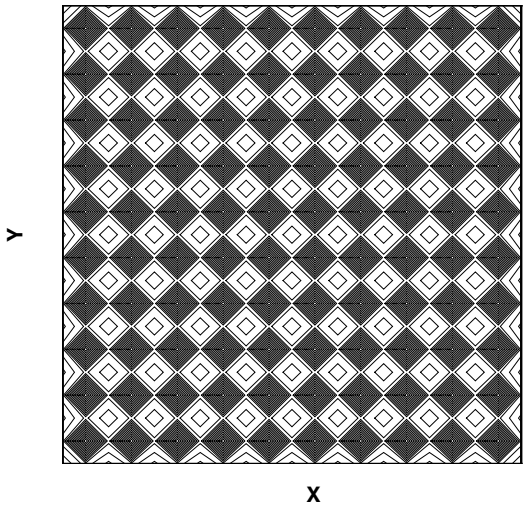

pressure contour

Figure 18 : A body force problem: MLPG with $\beta = 0$ (21×21 nodes and $r = 1.3h$).

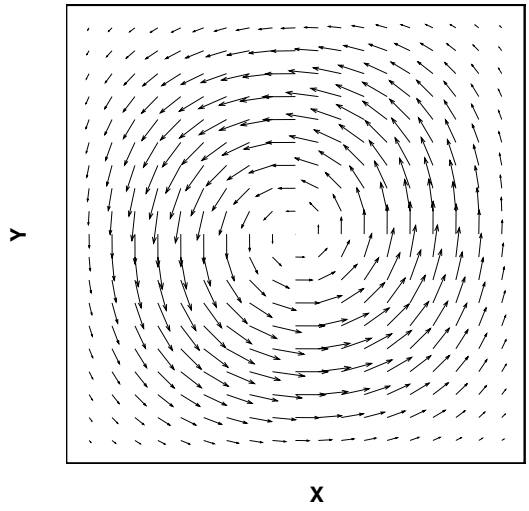

velocity field

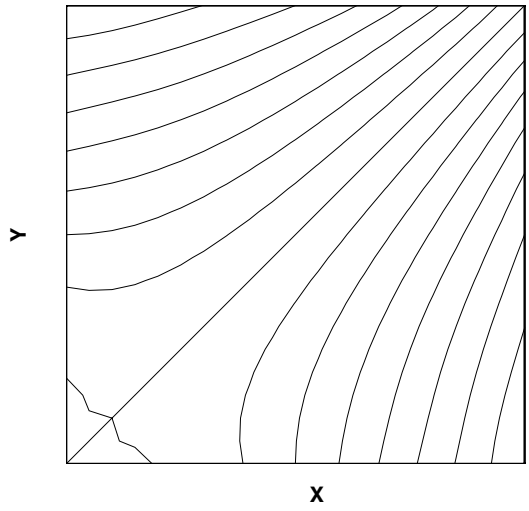

pressure contour

Figure 19 : A body force problem: MLPG with $\beta = 1$ (21×21 nodes and $r = 1.3h$).

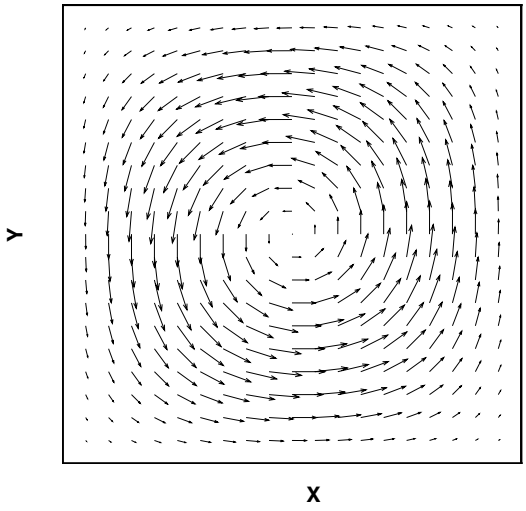

velocity field

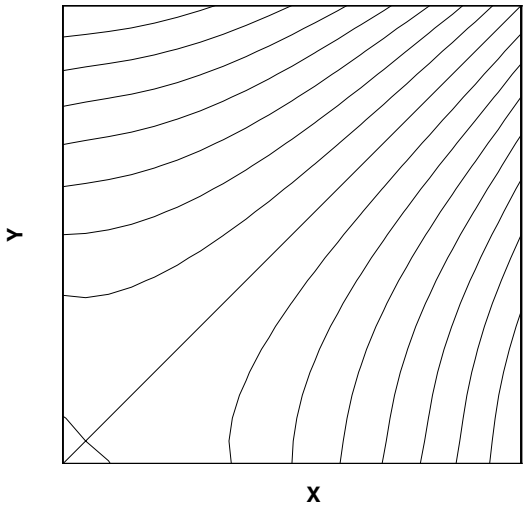

pressure contour

Figure 20 : A body force problem: MLPG with $\beta = 0.1$ (21×21 nodes and $r = 1.3h$).

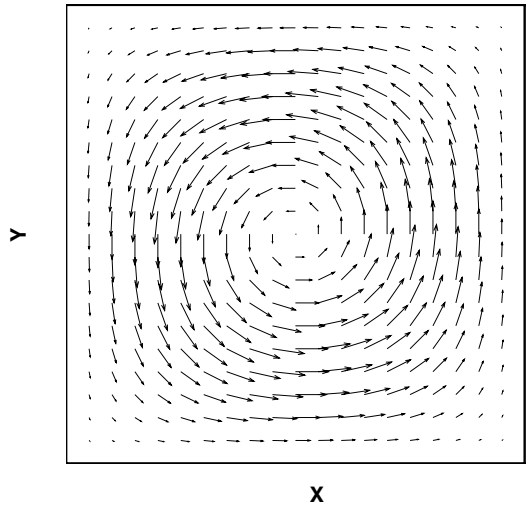

velocity field

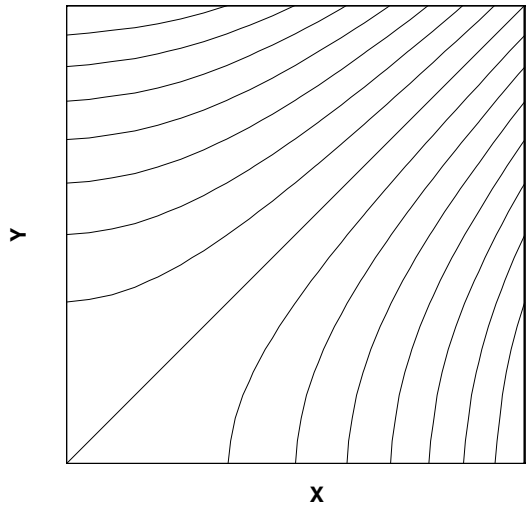

pressure contour

Figure 21 : A body force problem: MLPG with $\beta = 0.01$ (21×21 nodes and $r = 1.3h$).

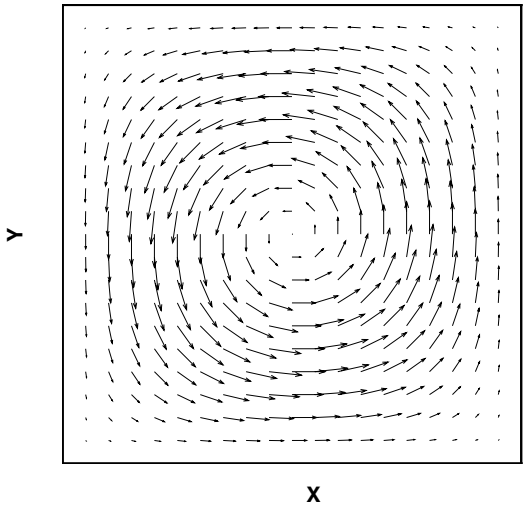

velocity field

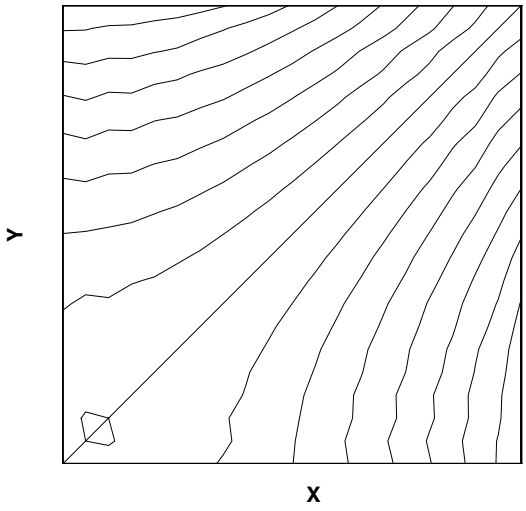

pressure contour

Figure 22 : A body force problem: MLPG with $\beta = 0.001$ (21×21 nodes and $r = 1.3h$).

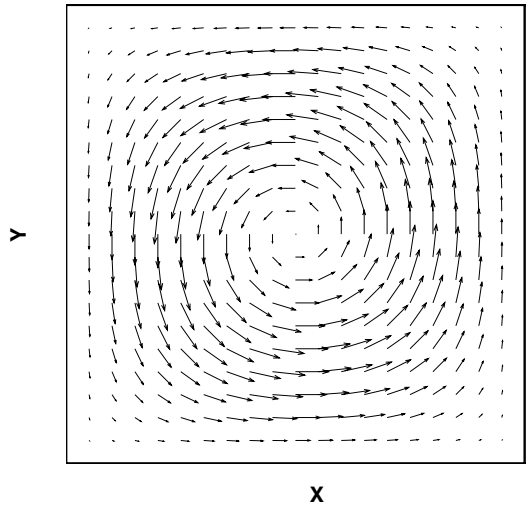

velocity field

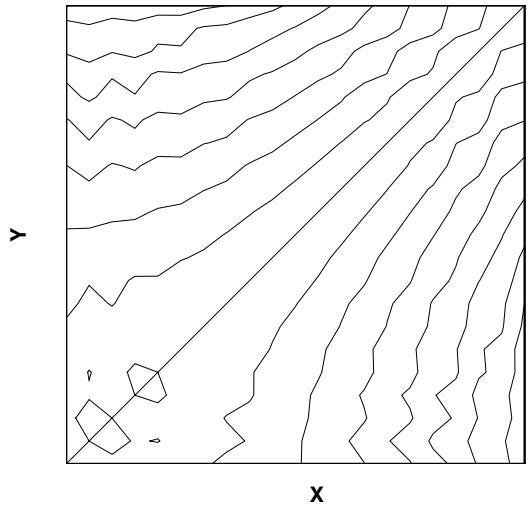

pressure contour

Figure 23 : A body force problem: MLPG with $\beta = 0.0001$ (21×21 nodes and $r = 1.3h$).

As in the previous example, different values for β are used and results are shown in Fig.24-Fig.29 for the MLPG method with 21×21 and radius of support $r = 1.3h$. No exact solutions can be obatined for this case.

Fig.24 show that, unlike the previous example, the MLPG method with the original mixed formulation ($\beta = 0$) not only gives highly oscillatory pressure results as before, but also produces bad results for velocity due to the singular boundary conditions. It also shows that when β becomes smaller, larger pressure oscillations will exhibit; when β becomes larger, both the velocity field and the pressure becomes more unreasonable. It looks the best choice for β is $\beta = 0.01$. Therefore, in the following calculation, β is chosen as $\beta = 0.01$. Again, good solutions demonstrate that ignoring the second order derivative term in Eq. (9) seems quite reasonable.

5.2 Steady-State Incompressible N-S Equations

Now we solve the general incompressible steady-state N-S equations. Due to the nonlinear convection term, iteration is necessary. The Newtonian iteration method is used here. To get convergent solutions, the starting solutions are important for the Newtonian iteration method. Here, the lid-driven cavity flow-through problem is solved with $Re = 100$ and $Re = 400$. For higher Reynolds number flows, better iteration schemes are necessary for convergence, which will be addressed in future. As shown in the case of Stokes flow, the parameter $\beta = 0.01$ is a good choice for the modified formulation. To deal with high Reynolds number flows, the upwinding schemes are necessary. Both the MLPG without upwinding and the MLPG with Upwinding Scheme II are used, and, as before, denoted as MLPG and MLPG2 respectively. 17×17 points and radius of support $r = 1.5h$ are used. Results for velocity and pressure fields are shown in Fig.30-Fig.31 show the results for $Re = 100$, and Fig.32-Fig.33 are solutions for $Re = 400$.

The results are quite good, although small oscillations still exist for pressure. Further investigation for the stability parameter τ is necessary. In addition, Fig.34 and Fig.35 show the results for u-velocity along vertical line and v-velocity along horizontal line through geometric center of cavity, compared with the classical results by Ghia, Ghia, and Shin (1982).

It shows that, for low Reynolds number flows, both MLPG and MLPG2 obtain very good solutions; for high Reynolds number flows, MLPG2 gives better solutions

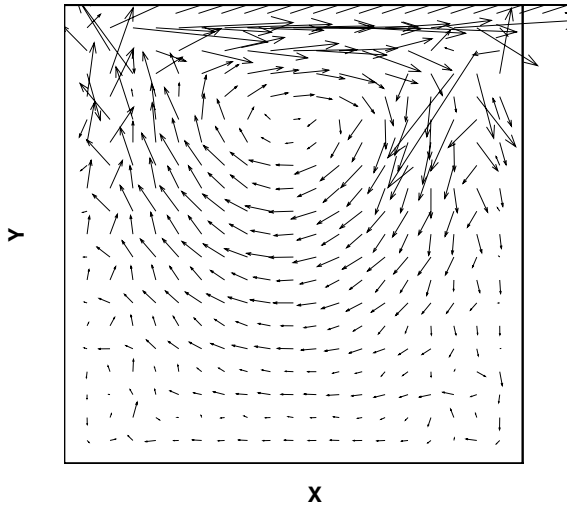

velocity field

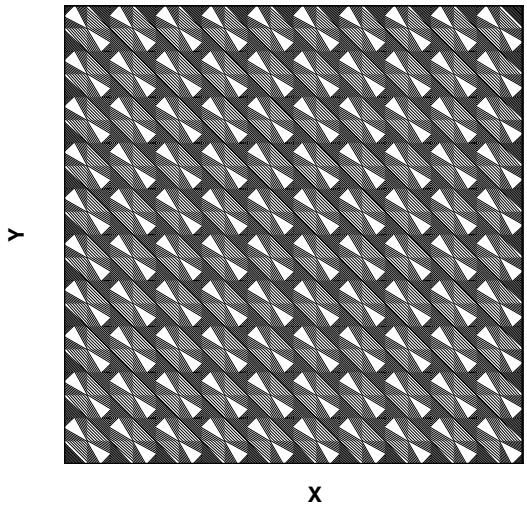

pressure contour

Figure 24 : Lid-driven cavity flow: MLPG with $\beta = 0$ (21×21 nodes and $r = 1.3h$).

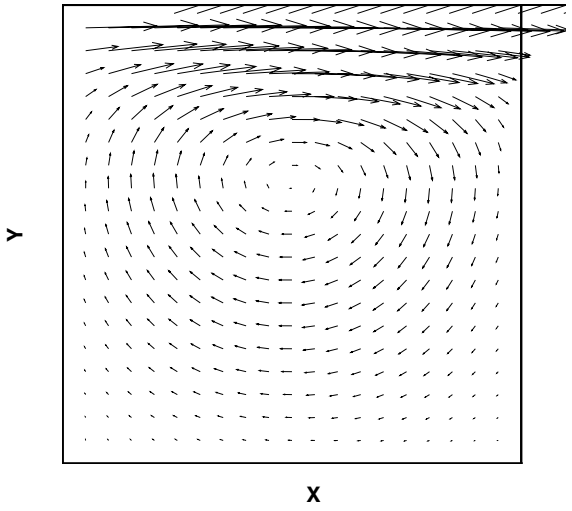

velocity field

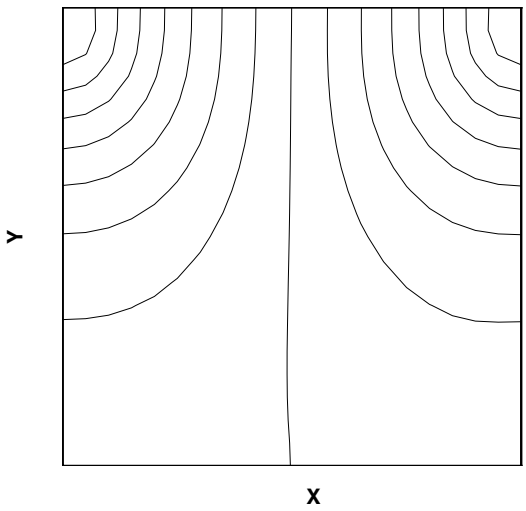

pressure contour

Figure 25 : Lid-driven cavity flow: MLPG with $\beta = 1$ (21×21 nodes and $r = 1.3h$).

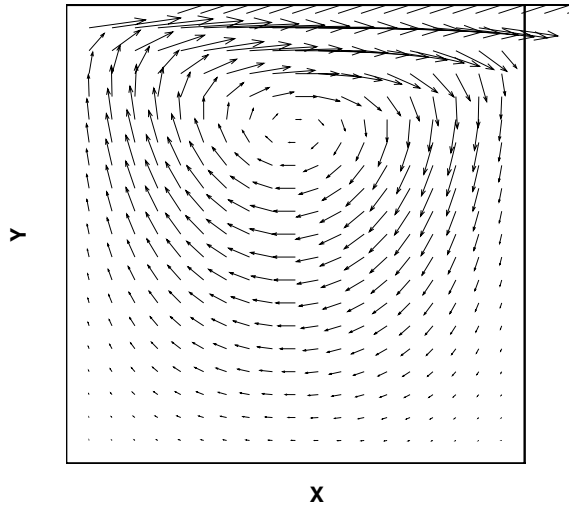

velocity field

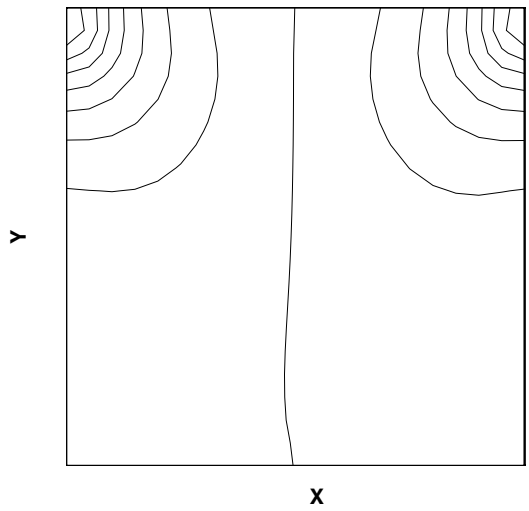

pressure contour

Figure 26 : Lid-driven cavity flow: MLPG with $\beta = 0.1$ (21×21 nodes and $r = 1.3h$).

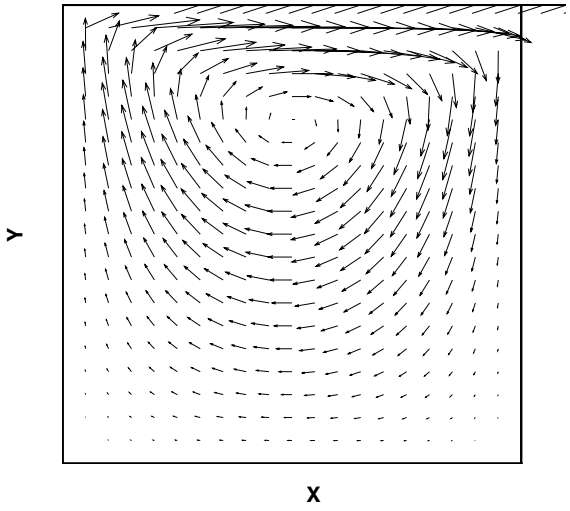

velocity field

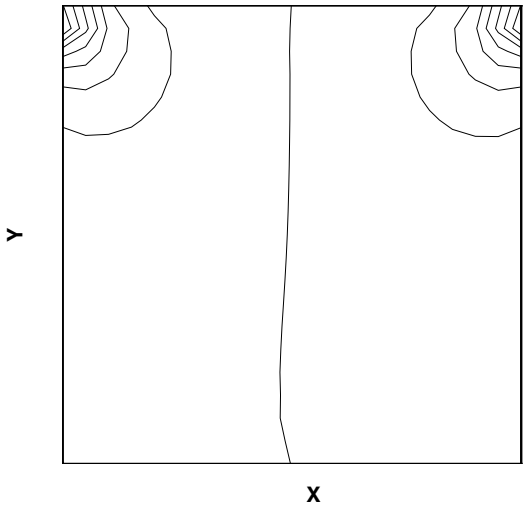

pressure contour

Figure 27 : Lid-driven cavity flow: MLPG with $\beta = 0.01$ (21×21 nodes and $r = 1.3h$).

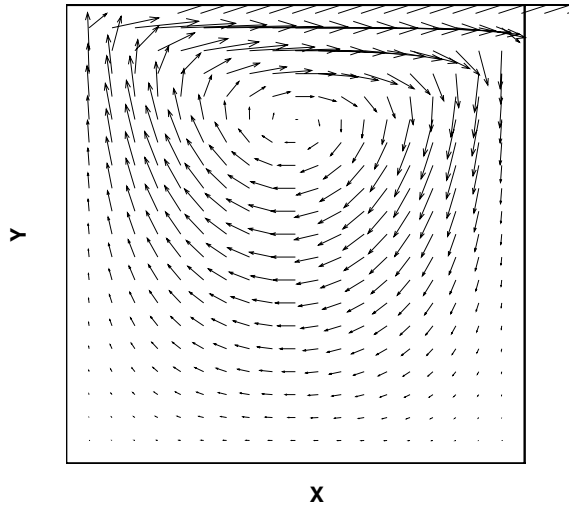

velocity field

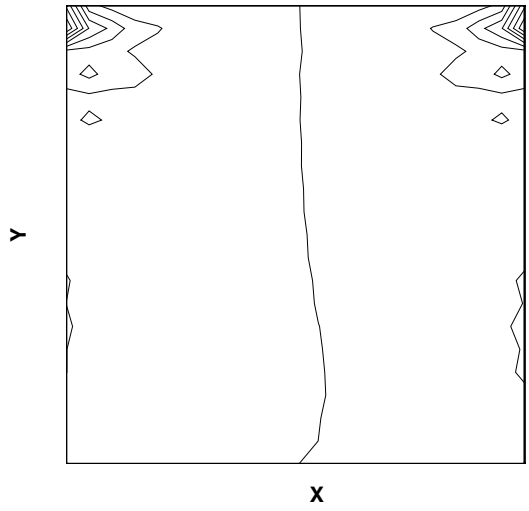

pressure contour

Figure 28 : Lid-driven cavity flow: MLPG with $\beta = 0.001$ (21×21 nodes and $r = 1.3h$).

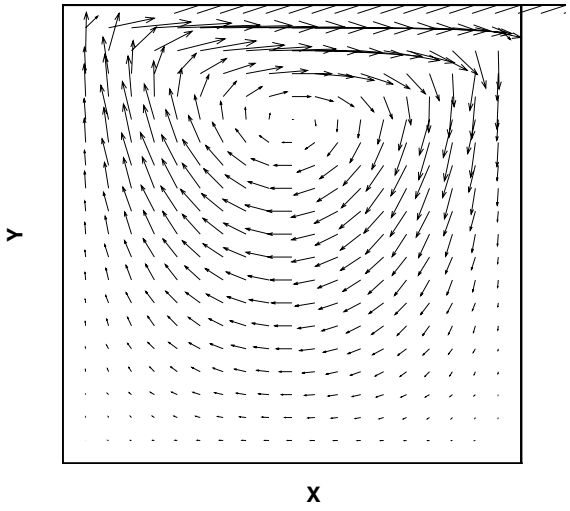

velocity field

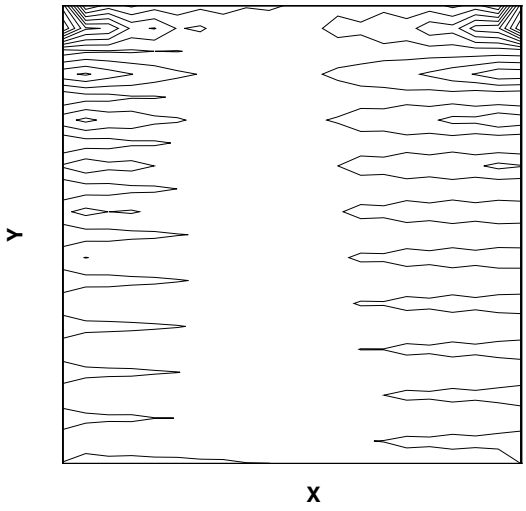

pressure contour

Figure 29 : Lid-driven cavity flow: MLPG with $\beta = 0.0001$ (21×21 nodes and $r = 1.3h$).

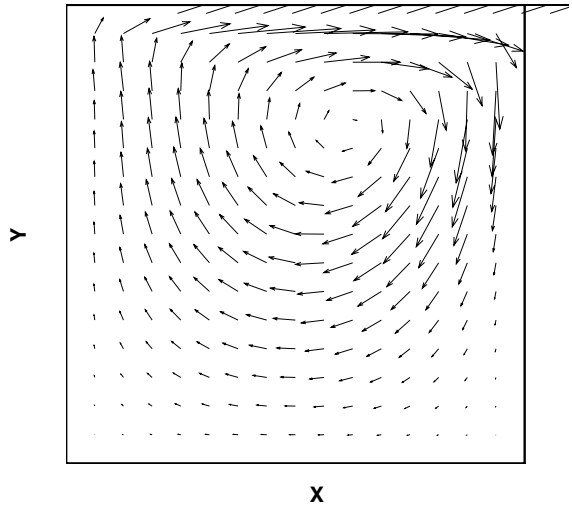

velocity field

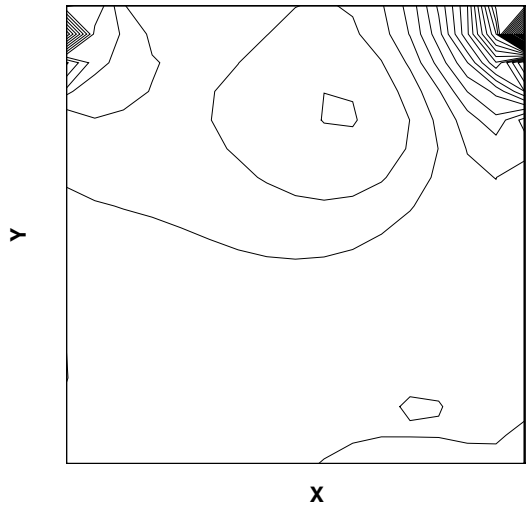

pressure contour

Figure 30 : Lid-driven cavity flow: MLPG with $Re = 100$ (17×17 nodes and $r = 1.5h$).

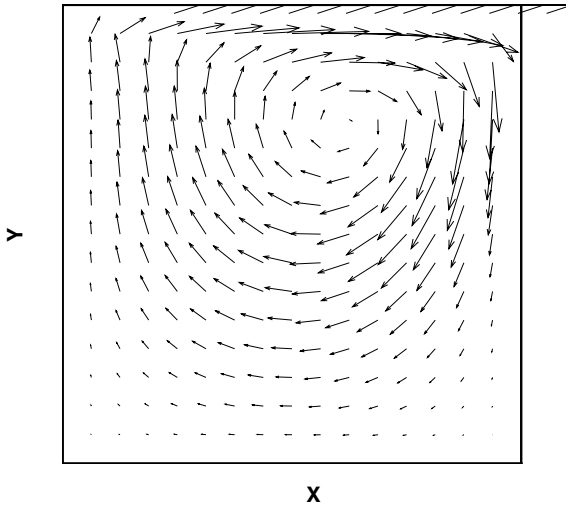

velocity field

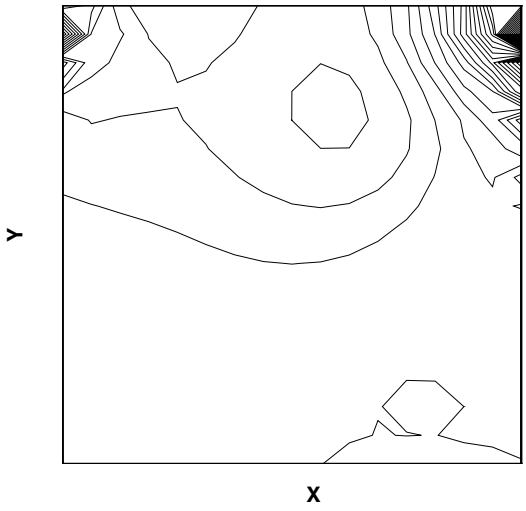

pressure contour

Figure 31 : Lid-driven cavity flow: MLPG2 with $Re = 100$ (17×17 nodes and $r = 1.5h$).

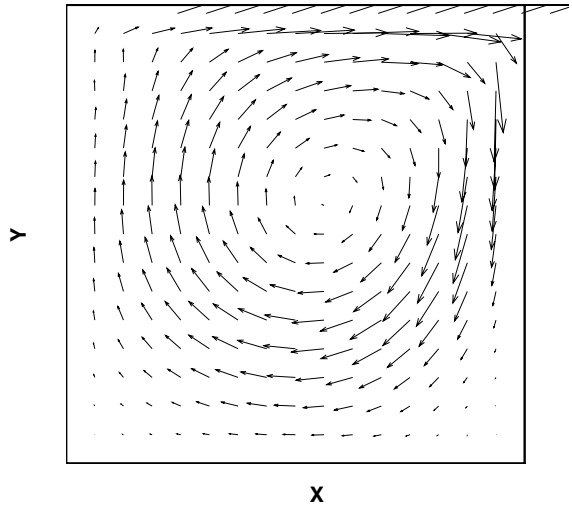

velocity field

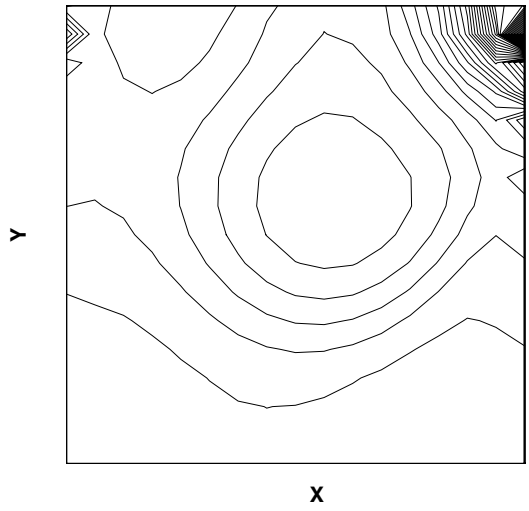

pressure contour

Figure 32 : Lid-driven cavity flow: MLPG with $Re = 400$ (17×17 nodes and $r = 1.5h$).

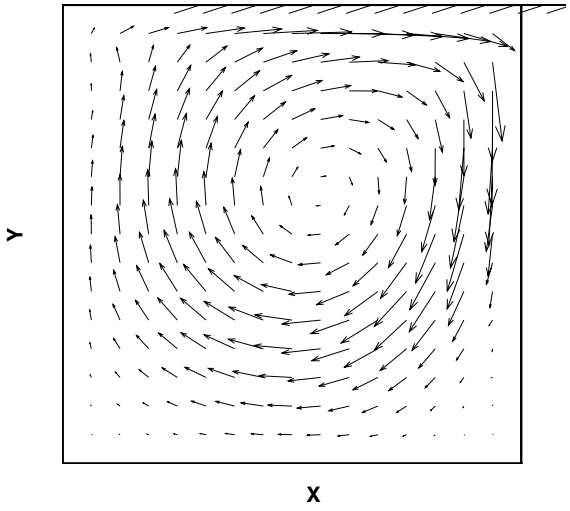

velocity field

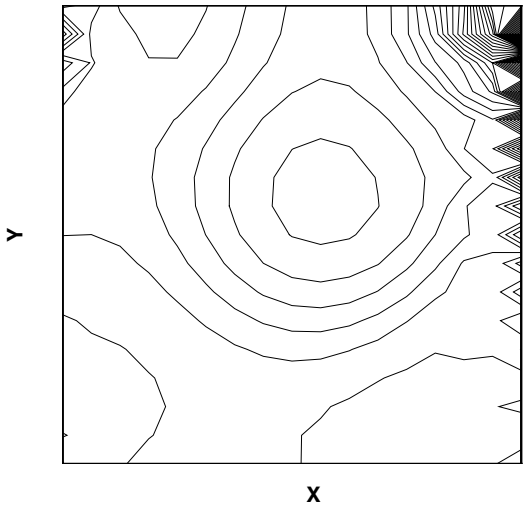

pressure contour

Figure 33 : Lid-driven cavity flow: MLPG2 with $Re = 400$ (17×17 nodes and $r = 1.5h$).

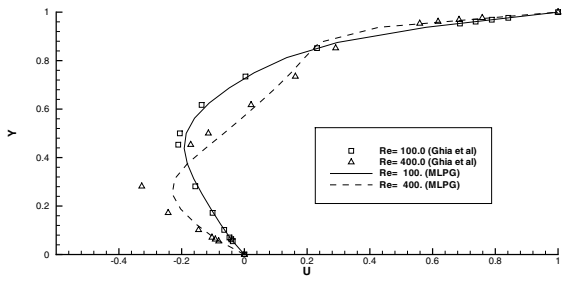

the MLPG without upwinding (MLPG)

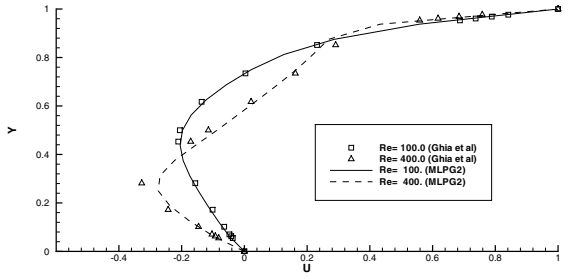

the MLPG with upwinding (MLPG2)

Figure 34 : Lid-driven cavity flow: Comparison of u-velocity along vertical lines through geometric center (17×17 nodes and $r = 1.5h$).

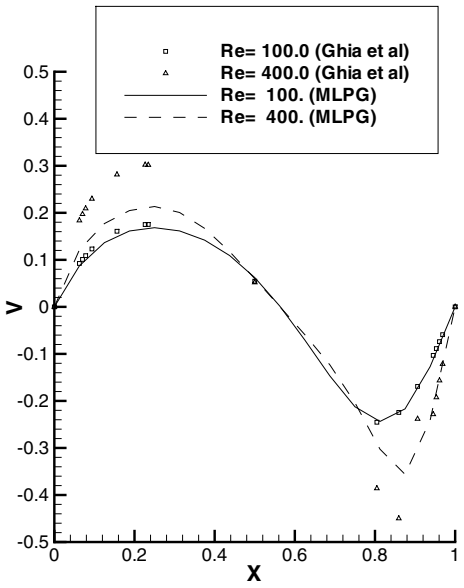

the MLPG without upwinding (MLPG)

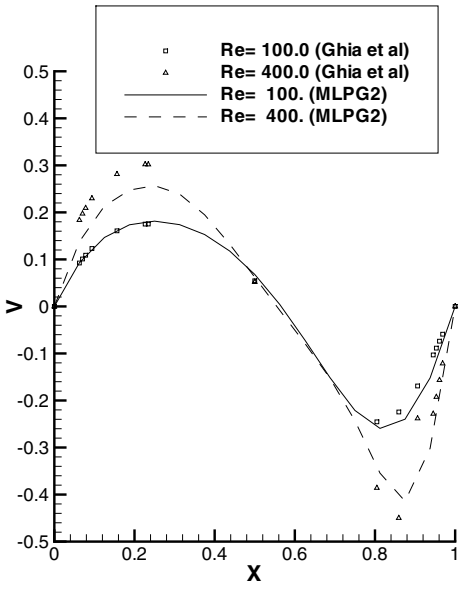

the MLPG with upwinding (MLPG2)

Figure 35 : Lid-driven cavity flow: Comparison of v-velocity along horizontal lines through geometric center (17×17 nodes and $r = 1.5h$).

than MLPG with the same number of points.

6 Conluding Remarks

In this paper, several classical problems related to the incompressible N-S equations are solved by using the MLPG method. One approach to overcome the so-called Babuška-Brezzi condition is proposed for the MLPG method. A 'perturbation' term is added into the standard mixed formulation for the purpose of stabilization without upsetting consistency. In order to reduce the cost, the second order derivative term in the modified mixed-formulation is omitted in the numerical implementation. Numerical results show that it works well for both the Stokes flows and the incompressible Navier-Stokes flows although further investigation is very important to determine the stability parameter τ.

In addition, the results for the incompressible N-S flows show that, the MLPG method with Upwinding Scheme II (US-II) leads to better performance for high Reynolds number flows, than the MLPG method without upwinding. It demonstrates that the MLPG method is very promising to solve the general fluid mechanics problems, and it may lead to a brand new solver due to its meshlessness and simplicity, although still some problems need to be addressed. Further studies will be done in future.

Acknowledgement: The support of this research by ONR and NASA-Langley is sincerely appreciated. Useful discussion with Drs. Y.D.S. Rajapakse and I.S. Raju are also thankfully acknowledged.

References

Atluri, S. N.; Cho, J. Y.; Kim, H. (1999): Analysis of thin beams, using the meshless local petrov-galerkin method, with generalized moving least squares interpolations. *Comput. Mech.*, vol. 24, pp. 334–347.

Atluri, S. N.; Kim, H.; Cho, J. Y. (1999): A critical assessment of the truly meshless local petrov-galerkin (mlpg), and local boundary integral equation (lbie) methods. *Comput. Mech.*, vol. 24, pp. 348–372.

Atluri, S. N.; Zhu, T. (1998a): A new meshless local petrov-galerkin (mlpg) approach in computational mechanics. *Comput. Mech.*, vol. 22, pp. 117–127.

Atluri, S. N.; Zhu, T. (1998b): A new meshless local petrov-galerkin (mlpg) approach to nonlinear problems

in computer modeling and simulation. *Computer Modeling and Simulation in Engrg.*, vol. 3, pp. 187–196.

Babuška, I. (1971): Error bounds for finite element method. *Numer. Math.*, vol. 16, pp. 322–333.

Babuška, I.; Melenk, J. (1997): The partition of unity method. *Int. J. Num. Meth. Eng.*, vol. 40, pp. 727–758.

Belytschko, T.; Krongauz, Y.; Organ, D.; Fleming, M.; Krysl, P. (1996): Meshless methods: an overview and recent developments. *Comput. Methods Appl. Mech. Engrg.*, vol. 139, pp. 3–47.

Belytschko, T.; Lu, Y. Y.; Gu, L. (1994): Element-free galerkin methods. *Int. J. Num. Meth. Eng.*, vol. 37, pp. 229–256.

Bratianu, C.; Atluri, S. N. (1983): A hybrid finite element method for Stokes flow. *Comput. Methods Appl. Mech. Engrg.*, vol. 36, pp. 23–37.

Brezzi, F. (1974): On the existence, uniqueness and approximation of saddle-point problems arising from Lagrange multipliers. *RAIRO Anal. Numer. (R-2)*, pp. 129–151.

Brezzi, F.; Bristeau, M. O.; Franca, L. P.; Mallet, M.; Roge, G. (1992): A relationship between stabilized finite element methods and the Galerkin method with bubble functions. *Comput. Methods Appl. Mech. Engrg.*, vol. 96, pp. 117–129.

Douglas, J.; Wang, J. (1989): An absolutely stabilized finite element method for the Stokes problem. *Math. Comp.*, vol. 52, pp. 495–508.

Duarte, C. A.; Oden, J. T. (1996): An h-p adaptive method using clouds. *Comput. Methods Appl. Mech. Engrg.*, vol. 139, pp. 237–262.

Fortin, M. (1981): Old and new finite element methods for incompressible flows. *Int. J. Num. Meth. Fluids*, vol. 1, pp. 347–364.

Franca, L. P.; Frey, S. L. (1992): Stabilized finite element methods: Ii. the incompressible Navier-Stokes equations. *Comput. Methods Appl. Mech. Engrg.*, vol. 99, pp. 209–233.

Franca, L. P.; Hughes, T. J. R. (1988): Two classes of mixed finite element methods. *Comput. Methods Appl. Mech. Engrg.*, vol. 69, pp. 89–129.

Franca, L. P.; Nesliturk, A.; Stynes, M. (1998): On the stability of residual-free bubbles for convection-diffusion problems and their approximation by a two-level finite element method. *Comput. Methods Appl. Mech. Engrg.*, vol. 166, pp. 35–49.

Franca, L. P.; Russo, A. (1996): Approximation of the Stokes problem by residual-free macro bubbles. *East-West J. Appl. Math.*, vol. 4, pp. 265–278.

Ghia, U.; Ghia, K. N.; Shin, C. T. (1982): High-re solutions for incompressible flow using the navier-stokes equations and a multigrid method. *J. Comput. Phys.*, vol. 48, pp. 387–411.

Hughes, T. J. R.; Franca, L. P. (1987): A new finite element formulation for computational fluid dynamics: VII. the Stokes problem with various well-posed boundary conditions: symmetric formulations that converge for all velocity/pressure spaces. *Comput. Methods Appl. Mech. Engrg.*, vol. 65, pp. 85–96.

Hughes, T. J. R.; Liu, W. K.; Brooks, A. (1979): Finite element analysis of incompressible viscous flows by the penalty function formulation. *J. Comput. Phys.*, vol. 30, pp. 1–60.

Lin, H.; Atluri, S. N. (2000a): Meshless Local Petrov-Galerkin (MLPG) method for convection-diffusion problems. *Computer Modeling in Engineering & Sciences*, vol. 1 (2), pp. 45–60.

Lin, H.; Atluri, S. N. (2000b): A truly Meshless Local Petrov-Galerkin (MLPG) approach for Burgers' equations. *Computer Modeling in Engineering & Sciences*. (In press).

Liu, W. K.; Jun, S.; Zhang, Y. (1995): Reproducing kernel particle methods. *Int. J. Num. Meth. Fluids*, vol. 20, pp. 1081–1106.

Lucy (1977): A numerical approach to the testing of the fission hypothesis. *The Astro. J.*, vol. 8, pp. 1013–1024.

Malkus, D. S.; Hughes, T. J. R. (1978): Mixed finite element methods - reduced and selective integration technique - a unification of concepts. *Comput. Methods Appl. Mech. Engrg.*, vol. 15, pp. 63–81.

Nayroles, B.; Touzot, G.; Villon, P. (1992): Generalizing the finite element method: diffuse approximation and diffuse elements. *Comput. Mech.*, vol. 10, pp. 307–318.

Oñate, E.; Idelsohn, S.; Zienkiewicz, O. C.; Taylor, R. L. (1996): A finite point method in computational mechanics. application to convective transport and fluid flow. *Int. J. Num. Meth. Eng.*, vol. 39, pp. 3839–3866.

Oden, J. T.; Jacquotte, O. P. (1984): Stability of some mixed finite element methods for Stokesian flows. *Comput. Methods Appl. Mech. Engrg.*, vol. 43, pp. 231–247.

Oden, J. T.; Kikuchi, N.; Song, Y. J. (1982): Penalty-finite element methods for the analysis of Stokesian flows. *Comput. Methods Appl. Mech. Engrg.*, vol. 31, pp. 297–329.

Pierre, R. (1988): Simple c^0 approximations for the computation of the incompressible flows. *Comput. Methods Appl. Mech. Engrg.*, vol. 68, pp. 205–227.

Sani, R. L.; Gresho, R. M.; Lee, R. L.; Griffiths, D. F. (1981): The cause and cure (?) of the spurious pressures generated by certain f.e.m. solutions of the incompressible navier-stokes equations, parts i and ii. *Int. J. Num. Meth. Fluids*, vol. 1, pp. 17–43; 171–204.

Stenberg, R. (1984): Analysis of mixed finite element methods for the Stokes problem: a unified approach. *Math. Comp.*, vol. 42, pp. 9–23.

Yang, C. T.; Atluri, S. N. (1984a): An 'assumed deviatoric stress-pressure-velocity' mixed finite element method for unsteady, convective, incompressible viscous flow: part I: theory. *Int. J. Num. Meth. Fluids*, vol. 4, pp. 43–69.

Yang, C. T.; Atluri, S. N. (1984b): An 'assumed deviatoric stress-pressure-velocity' mixed finite element method for unsteady, convective, incompressible viscous flow: part II: computational studies. *Int. J. Num. Meth. Fluids*, vol. 4, pp. 43–69.

Zhu, T.; Atluri, S. N. (1998): A modified collocation & a penalty formulation for enforcing the essential boundary conditions in the element free galerkin method. *Comput. Mech.*, vol. 21, pp. 211–222.

Zhu, T.; Zhang, J. D.; Atluri, S. N. (1998a): A local boundary integral equation (lbie) method in computational mechanics, and a meshless discretization approach. *Comput. Mech.*, vol. 21, pp. 223–235.

Zhu, T.; Zhang, J. D.; Atluri, S. N. (1998b): A meshless local boundary integral equation (lbie) method for solving nonlinear problems. *Comput. Mech.*, vol. 22, pp. 174–186.